Divergent neural circuits for proprioceptive and exteroceptive sensing of the *Drosophila* leg

Su-Yee J. Lee[1], Chris J. Dallmann[1,2], Andrew Cook[1], John C. Tuthill[1*], Sweta Agrawal[1,3,*]
[1] Department of Physiology and Biophysics, University of Washington, Seattle, WA, USA
[2] Department of Neurobiology and Genetics, Julius-Maximilians-University of Würzburg, Würzburg, Germany
[3] School of Neuroscience, Virginia Tech, Blacksburg, VA, USA
*Correspondence: tuthill@uw.edu, sweta@vt.edu

Abstract

Somatosensory neurons provide the nervous system with information about mechanical forces originating inside and outside the body. Here, we use connectomics from electron microscopy to reconstruct and analyze neural circuits downstream of the largest somatosensory organ in the *Drosophila* leg, the femoral chordotonal organ (FeCO). The FeCO has been proposed to support both proprioceptive sensing of the fly's femur-tibia joint and exteroceptive sensing of substrate vibrations, but it was unknown which sensory neurons and central circuits contribute to each of these functions. We found that different subtypes of FeCO sensory neurons feed into distinct proprioceptive and exteroceptive pathways. Position- and movement-encoding FeCO neurons connect to local leg motor control circuits in the ventral nerve cord (VNC), indicating a proprioceptive function. In contrast, signals from the vibration-encoding FeCO neurons are integrated across legs and transmitted to mechanosensory regions in the brain, indicating an exteroceptive function. Overall, our analyses reveal the structure of specialized circuits for processing proprioceptive and exteroceptive signals from the fly leg. These findings are consistent with a growing body of work in invertebrate and vertebrate species demonstrating the existence of specialized limb mechanosensory pathways for sensing external vibrations.

Introduction

To coordinate complex behaviors, circuits in the central nervous system (CNS) require continuous information about the body and the environment. An important source of feedback are somatosensory neurons, which provide the nervous system with information about mechanical forces acting on an animal's body[1,2]. Somatosensory neurons are typically described as either exteroceptive, detecting mechanical forces generated in the external world, or proprioceptive, detecting the position or movement of body parts. However, because they are embedded within the body, many somatosensory neurons can detect both externally- and self-generated forces, making it difficult to determine whether specific somatosensory neurons are exteroceptive, proprioceptive, or both. Recording from primary somatosensory neurons in behaving animals can resolve the types of mechanical stimuli they encode[3], but such experiments are

technically difficult and often not feasible. An alternative approach is to map the connectivity of sensory neurons with downstream circuits, which can provide clues about putative function. For example, proprioceptor axons often synapse directly onto motor neurons to support rapid reflexes[4] (**Figure 1A**). In contrast, exteroceptive signals are often integrated with other sensory cues and modified by internal states to more flexibly control action selection[5,6].

Mapping the flow of sensory signals into the nervous system has recently become feasible in small organisms thanks to advances in serial-section electron microscopy (EM) and computational image segmentation, which enable the reconstruction of synaptic wiring diagrams, or connectomes. Some of the most comprehensive wiring diagrams reconstructed to date include the brain and ventral nerve cord (VNC) of the adult fruit fly, *Drosophila melanogaster*[7–11]. Analysis of fly brain connectome datasets has already produced important insight into the organization and function of sensory organs on the head. For example, mapping the projections of mechanosensory neurons from the fly's antennae into the brain revealed the organization of circuits that support song detection, antennal grooming, and escape[12,13]. Volumetric EM datasets of the fly VNC[8,9], which is analogous to the vertebrate spinal cord, now make it possible to reconstruct and analyze the function of somatosensory signals from other parts of the fly's body, including the legs and wings.

Here, we take advantage of two separate connectome datasets that together span the CNS of a fruit fly, the Female Adult Nerve Cord (FANC)[8,14] and the Full Adult Fly Brain (FAFB), which was reconstructed as part of FlyWire[7,15]. We use connectomic analyses of brain and VNC circuits to investigate the largest somatosensory organ in the *Drosophila* leg, the femoral chordotonal organ (FeCO) (**Figure 1B**). The cell bodies and dendrites of the FeCO are located in the femur of each leg and their axons project into the VNC (**Figure 1B)**[16–19]. The *Drosophila* FeCO is comprised of ~150 excitatory (cholinergic) sensory neurons that can be separated into five functionally and anatomically distinct subtypes: (1) extension- and (2) flexion-encoding claw neurons encode tibia position, (3) extension- and (4) flexion-encoding hook neurons encode tibia movement, and (5) club neurons encode bidirectional tibia movement and low-amplitude (<1 µm), high-frequency tibia vibration (**Figure 1C-D**)[18,19]. Claw, hook, and club neurons are named after the shape of their axons in the VNC (**Figure 1E**).

The FeCO is typically described as a proprioceptive organ that monitors the movement and position of the femur-tibia joint[18–20]. However, behavioral evidence suggests that it may also detect externally-generated substrate vibrations, perhaps to aid in social communication, predator detection, and courtship[21–24]. It is currently unknown to what degree the five subtypes of FeCO sensory neurons are specialized to support specific proprioceptive or exteroceptive functions. The club neurons are the only FeCO subtype that respond to tibia vibration (**Figure 1D**), suggesting that they could support exteroceptive vibration

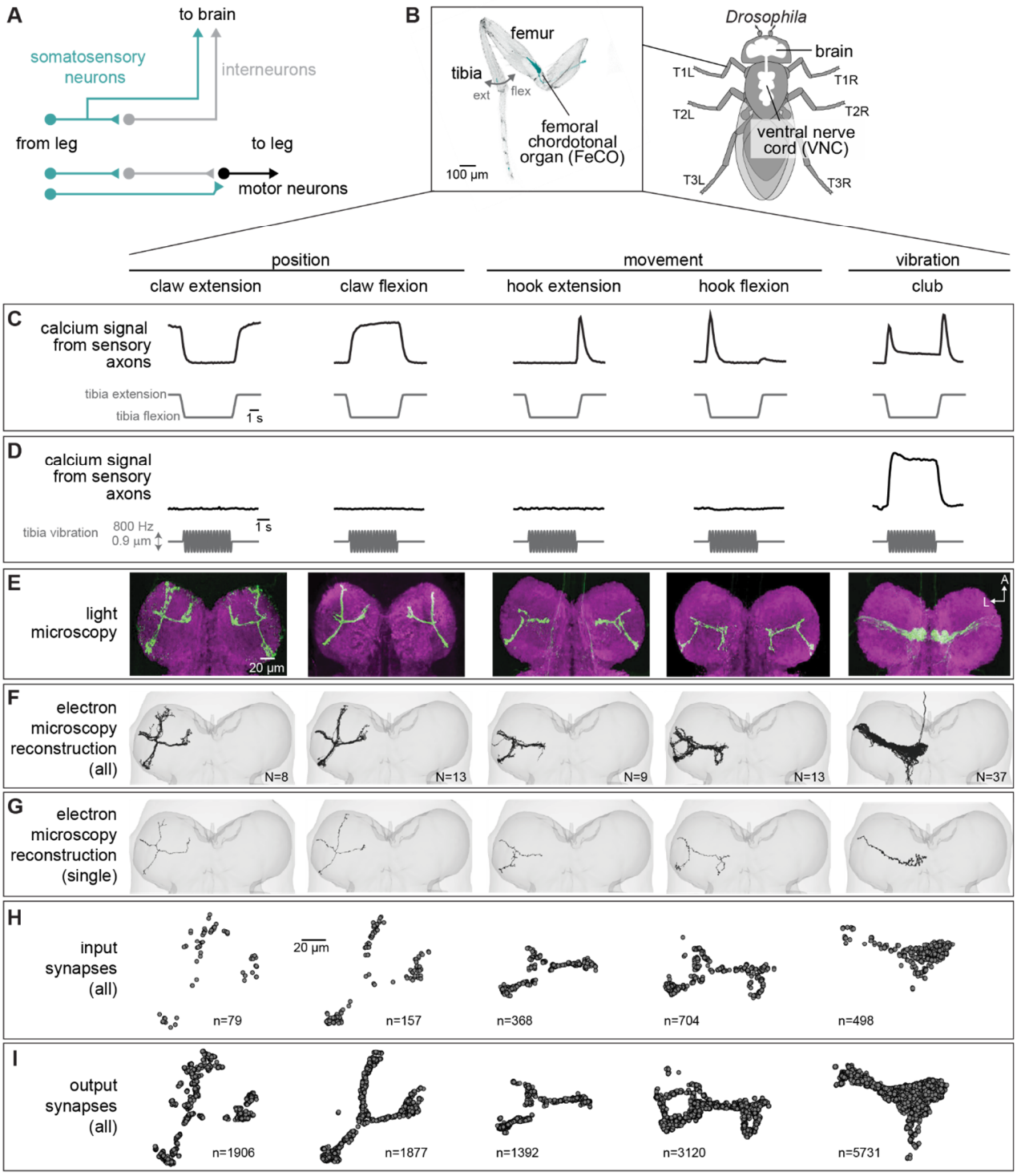

Figure 1. Connectomic reconstruction of axonal projections from somatosensory neurons in the femoral chordotonal organ (FeCO) of a female *Drosophila.* (**A**) Schematic of local and ascending VNC circuits for leg somatosensation and motor control. (**B**) Left: Confocal image of a *Drosophila* front leg showing the location of FeCO cell bodies and dendrites. Green: GFP; gray: cuticle auto-fluorescence. Right: Schematic showing the fly brain and ventral nerve cord (VNC) (C-I) Anatomical and functional subtypes of somatosensory neurons in the *Drosophila* FeCO. (**C**) Calcium signals from FeCO axons of each subtype (GCaMP, black traces) in response to a controlled movement of the femur-tibia joint (gray traces). Adapted from Mamiya et al., (2023). (**D**) Calcium signals from FeCO axons of each subtype (GCaMP, black traces) in response to an 800 Hz vibration of the femur-tibia joint (gray traces). Adapted from Mamiya et al., (2023). (**E**) Confocal images of the axons of each FeCO subtype in the fly ventral nerve cord (VNC). Green: GFP; magenta: neuropil stain (nc82). Adapted from Agrawal et al., (2020) A: anterior; L: lateral. (**F**) Reconstructed FeCO axons from each subtype in the front left leg neuromere of the FANC connectome (from left to right, N=8, 13, 9, 13, 37 neurons). (**G**) Single reconstructed axons from each FeCO subtype in the front left leg neuromere of the FANC connectome. (**H**) Locations of all input synapses received by each FeCO subtype (i.e. postsynaptic sites). *n* indicates the number of synapses. (**I**) Locations of all output synapses made by each FeCO subtype (i.e. presynaptic sites). n indicates the number of synapses.

70 sensing[18,19]. However, club neurons also respond to larger tibia movements like those that occur during
71 walking (**Figure 1C**), suggesting that they could also be proprioceptive. Intracellular recordings from
72 second-order neurons have identified distinct pathways for proprioceptive and vibration sensing, but in
73 some cases also revealed complex pooling of signals from multiple FeCO subtypes[25,26].

74 Here, we use the FANC[14] and FlyWire[7,15] connectome datasets to reconstruct and analyze neural
75 circuits downstream of the FeCO of the fly's front left (T1L) leg. We find that position- and movement-
76 encoding claw and hook neurons connect to local circuits within the VNC for leg motor control, confirming
77 their proprioceptive function. In contrast, vibration-encoding club neurons connect to intersegmental and
78 ascending circuits that integrate mechanosensory information from the legs, wings, and neck, and relay it
79 to the brain. By identifying these ascending projections within the FlyWire connectome, we find neurons
80 within the brain that integrate leg vibration information with mechanosensory information from the
81 antennae, indicating an exteroceptive function for club neurons. We also identify sparse pathways that
82 mediate interactions between proprioceptive and exteroceptive circuits, revealing how vibration signals
83 may directly influence motor output. Overall, our analyses suggest that the FeCO supports both
84 proprioceptive and exteroceptive functions, which are achieved via specialized somatosensory neurons
85 connected to specialized downstream circuits.
86

87 **Results**

88 **Reconstruction and identification of FeCO axons in the FANC connectome**

89 Using software for collaborative proofreading and visualization of the FANC EM dataset (see Methods),
90 we reconstructed the anatomy and synaptic connectivity of FeCO axons from the front left leg. We focused
91 our reconstruction efforts on these FeCO axons because they project to the front left neuromere of the VNC
92 (also referred to as left T1 or T1L), the region of the *Drosophila* VNC with the most complete information
93 about leg sensorimotor circuits. All of the motor neurons controlling the muscles of the front left leg and
94 their presynaptic partners have been previously identified and reconstructed in FANC[14,27], and prior
95 neurophysiological recordings of FeCO axons and their downstream targets were made from the front
96 legs[18,19,25,26,28,29]. Unfortunately, leg sensory axons are among the most difficult neurons to reconstruct in
97 all available VNC connectome datasets, likely due to rapid degeneration that begins when the legs are
98 dissected away from the VNC during sample preparation. Leg sensory neurons have consistently darker
99 cytoplasm and more fragmented cell membranes, leading to poor automatic neuron segmentations and
100 synapse predictions. As a result, we reconstructed roughly half[18,19] of the FeCO axons from the front left
101 leg (80 total axons, **Figure 1F-I**). For comparison, the other publicly available VNC connectome dataset,
102 MANC (v.1.2.1), had only 22 T1L FeCO axons reconstructed and many of these were incomplete and

missing branches. We found that the number of novel postsynaptic partners decreased as we added more axons to the dataset (**Figure S1A**), suggesting that our reconstruction, while incomplete, provides a representative sample of the postsynaptic circuitry.

The FeCO consists of five functional subtypes (**Figure 1C-D**)[19]. We sorted the reconstructed FeCO axons into these functional subtypes based on axon morphology and comparison with light microscopy images (**Figure 1E-G**; see Methods). Based on measurements of the number of FeCO cell bodies in the leg[19], we estimate that we reconstructed ~50% of the T1L axons of each subtype (**Supplemental Table 1**). EM reconstructions of axons from each subtype qualitatively matched previous light-level images[18], including 5 club axons from the T1L leg that send an ascending projection to the brain. As expected for sensory neurons, all FeCO axons have more presynaptic sites (i.e., output synapses) than postsynaptic sites (i.e. input synapses) (**Figure 1H-I, Figure S1C-E**). Generally, the locations of pre- and postsynaptic sites are intermingled; FeCO axons do not have distinct pre- and postsynaptic zones. Finally, we do not find strong evidence for functional specialization of the different sub-branches of hook or claw neurons. Most postsynaptic neurons receive input from multiple branches (**Figure S2**).

Claw and hook (but not club) axons provide feedback to local leg motor circuits

To investigate pathways downstream of the different FeCO subtypes, we reconstructed the anatomy and synaptic connectivity of all postsynaptic partners that receive at least 4 synapses from a FeCO axon, a threshold found by previous studies to mitigate the inclusion of false positives due to errors in synapse prediction[7,30] and bias analyses towards stereotyped connections that consistently appear across multiple datasets[15]. We classified all postsynaptic VNC neurons into six morphological classes: (1) descending and (2) ascending neurons that connect the brain and VNC, (3) intersegmental neurons, which span multiple VNC neuromeres, (4) local neurons located entirely in the T1L neuromere, (5) motor neurons, and (6) sensory neurons (**Figure 2A**). We interpret connectivity of FeCO axons with local interneurons or leg motor neurons as suggesting a role in local, rapid feedback control of leg motor output. In contrast, we interpret connectivity with ascending neurons as suggesting a role in mediating sensation and behavior on longer timescales, such as sensory perception and action selection.

We found that the majority of synapses from claw and hook extension axons are onto local VNC interneurons and leg motor neurons (**Figure 2B-C**). In contrast, more than half of all synapses from club axons are onto intersegmental neurons. Hook flexion axons are somewhere in between, making roughly similar proportions of their synapses onto local and intersegmental postsynaptic partners. Club and hook flexion axons also make a notably high number of synapses onto ascending neurons that convey leg somatosensory information to the brain.

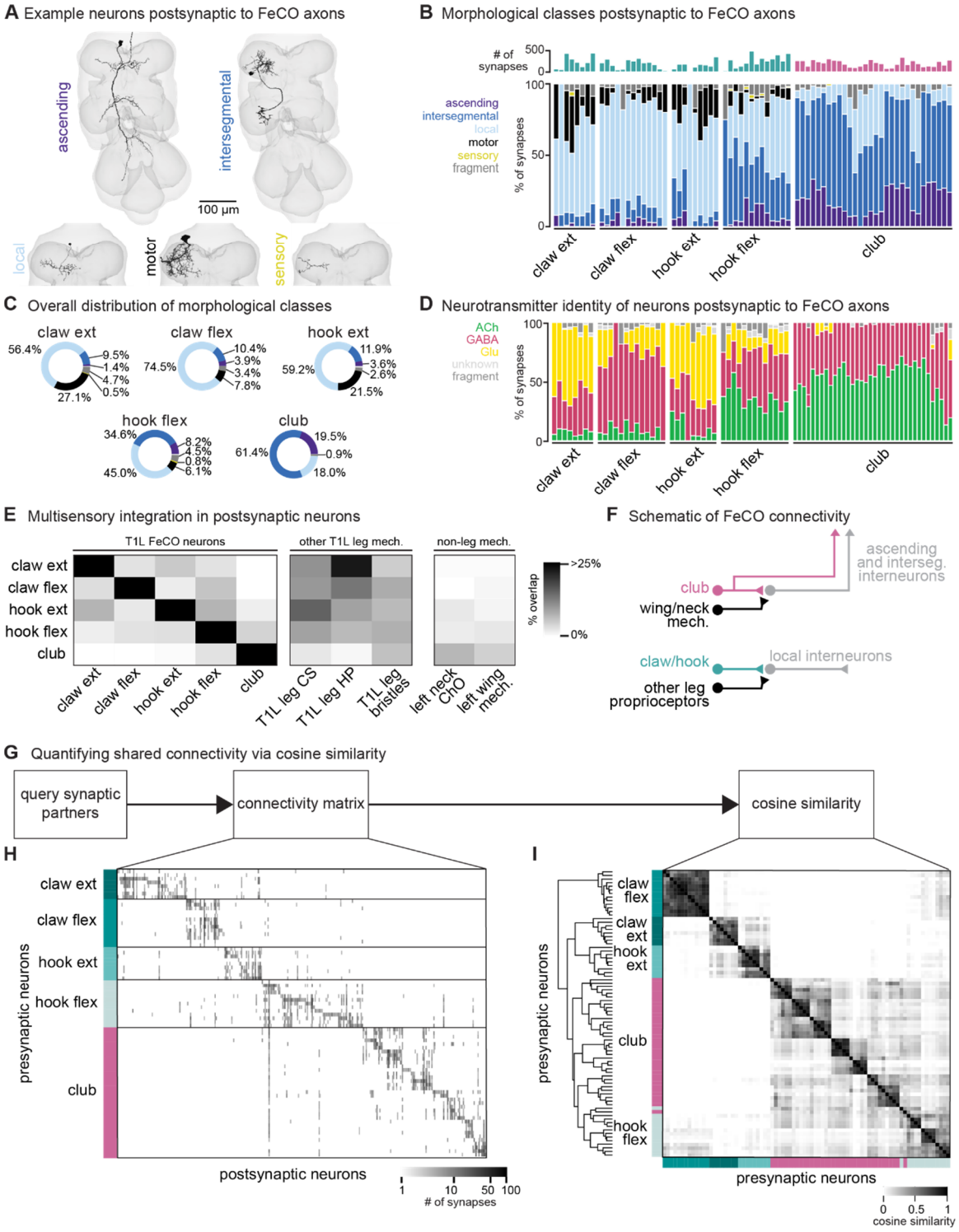

Figure 2. FeCO neurons exhibit subtype-specific postsynaptic connectivity. (**A**) We reconstructed all VNC neurons postsynaptic to FeCO axons from the front left leg (T1L) and classified them into morphological classes. Example provided from each class. (**B**) Percent of synapses from each FeCO axon that are made onto VNC neurons of each morphological class. Top bar plot shows the total number of output synapses made by each FeCO axon. (**C**) Per FeCO subtype, the total fraction of output synapses made onto each morphological class. (**D**) Proportion of total synapses made by each FeCO neuron onto cholinergic (green), glutamatergic (yellow), GABAergic (pink), and unidentified (light gray) hemilineages. (**E**) Heatmap shows the percent of neurons postsynaptic to a particular T1L FeCO subtype (as indicated along the rows) that also receive synaptic input from an alternate somatosensory population: T1L FeCO neurons, including claw extension axons, claw flexion axons, hook extension axons, hook flexion axons, or club axons, other T1L leg mechanosensory neurons, including campaniform sensilla axons (CS), hair plate axons (HP), or bristle axons, and non-leg somatosensory neurons, including left neck chordotonal organ axons or left wing somatosensory axons. We found that neurons postsynaptic to claw and hook axons also integrate information from other leg proprioceptors such as HP axons and CS axons. In contrast, neurons postsynaptic to club axons do not integrate information from other leg proprioceptors, but they do integrate information from wing and neck somatosensory axons. (**F**) Schematic of FeCO connectivity. Club information is conveyed primarily to ascending and intersegmental neurons, who also receive information from wing and neck somatosensory neurons. (legend contd. on next page)

(Fig. 2 legend continued) Information from claw and hook axons is primarily relayed to local interneurons, which also receive information from other leg proprioceptive neurons. (**G**) By querying the connectivity of each postsynaptic partner of each reconstructed FeCO neuron, we obtained H) a connectivity matrix and I) a cosine similarity matrix. (H) Connectivity matrix between FeCO axons and postsynaptic VNC neurons. The shading of each tick indicates the number of synapses from each FeCO axon (row) onto each postsynaptic VNC neuron (column). Colored bars along the left indicate the presynaptic FeCO subtype for that row. FeCO axons are organized by morphological subtype and then by their cosine similarity scores. VNC neurons are organized by their cosine similarity scores. (I) Clustered pairwise cosine similarity matrices of all FeCO axons based on their postsynaptic connectivity. The cosine similarity between two neurons is the dot product of the normalized (unit) column weight vectors. If two FeCO neurons synapse with similar synaptic weights onto the same postsynaptic neuron, relative to the FeCO's total output, the pairwise cosine similarity is 1. FeCO neurons with similar postsynaptic connectivity patterns cluster together, forming connectivity clusters.

We next used anatomical criteria to identify the developmental origins of all pre- and postsynaptic partners of FeCO axons (see Methods). About 95% of adult neurons in the *Drosophila* VNC arise from 30 segmentally repeated neuroblasts (neural stem cells), each of which divides to form an 'A' and 'B' hemilineage[31]. Developmental hemilineages are an effective means to classify VNC cell types: neurons of the same hemilineage release the same primary neurotransmitter (i.e., Lacin's law)[32,33] and express similar transcription factors[34,35]. Previous research also suggests that neurons within a hemilineage are functionally related: thermogenetic activation of single hemilineages drove leg and wing movements[36], and connectome analyses of larval VNC neurons demonstrated that neurons within a hemilineage share common synaptic partners[37].

We found that club axons target neurons from different hemilineages than claw and hook axons (**Figure S3,** see **Supplemental Table 2** for links to view entire populations of each hemilineage in Neuroglancer). Neurons that are primarily postsynaptic to club axons come from hemilineages 0A/0B, 1B, 8B, 9A, 10B, and 23B. Of those, only 1B and 9A neurons receive any synaptic input from claw axons, but the connectivity is weak (~6% and 0.5% of total FeCO input, respectively). Club and hook flexion axons target some shared hemilineages, including 1B, 9A, and 23B. Neurons from all other identified hemilineages are predominantly postsynaptic to claw or hook axons and do not receive any synaptic input from club axons. We further used the hemilineage designations to infer a neuron's primary neurotransmitter (**Figure 2D**). The majority of *Drosophila* neurons release one of three primary neurotransmitters: acetylcholine, GABA, or glutamate[34,38]. In the fly, acetylcholine is typically excitatory, while GABA is typically inhibitory[34,39,40]. Glutamate is excitatory at the fly neuromuscular junction, acting on ionotropic glutamate receptors (GluRs), but is frequently inhibitory in the CNS, acting on the glutamate-gated chloride channel, GluCl[41]. Club axons synapse onto very few putative glutamatergic neurons compared to claw and hook axons (**Figure 2D**).

We conducted similar analyses examining the presynaptic inputs to FeCO axons (**Figure S4**). Generally, hook axons receive the most input synapses and have the most presynaptic partners, which include local, ascending, and intersegmental neurons (**Figure S4A-B**). The majority of input synapses to FeCO axons are GABAergic (**Figure S4D**). The strongest input comes from 9A neurons, which are primarily presynaptic to hook axons (**Figure S3C-D**). Recent work found that a subset of 9A neurons

suppress expected proprioceptive feedback from hook neurons during voluntary movements such as walking or grooming[29].

Together, these differences in postsynaptic connectivity suggest that claw and hook axons are connected to postsynaptic partners that are distinct from those downstream of club axons. These downstream partners differ in their morphology as well as their developmental stem-cell lineage. Hook and claw axon connectivity with local and motor neurons suggests that they play a role in fast feedback control of leg motor output. In contrast, club axons connect to intersegmental and ascending pathways that could relay leg vibration information to the brain to support detection of external mechanosensory signals (**Figure 2F**). In support of this conclusion, we found that the VNC neurons that receive input from claw and hook axons also receive input from other leg proprioceptors, such as hair plate and campaniform sensilla neurons. In contrast, the VNC neurons that receive input from club axons receive little input from leg proprioceptors but instead receive sizeable input from somatosensory neurons on the neck and wing (**Figure 2E-F**).

FeCO axons demonstrate subtype-specific downstream connectivity

We next investigated the specific postsynaptic partners targeted by claw, hook, and club axons and the degree to which FeCO axons synapse onto distinct or overlapping circuits. First, we constructed a connectivity matrix to look at the postsynaptic connectivity of each FeCO neuron, organizing the rows of the matrix by FeCO subtype (**Figure 2G-H**). Generally, postsynaptic connectivity is sparse, with each FeCO neuron contacting 21.1 ± 1.1 (mean ± s.e.m.) distinct postsynaptic partners (**Figure S1B**). To quantify this connectivity structure, we calculated the cosine similarity score for pairs of FeCO axons based on their synaptic outputs (**Figure 2I**; see Methods). Two FeCO axons have a high cosine similarity score if they make the same relative number of synapses onto the same postsynaptic neurons. Low similarity scores indicate either that two FeCO axons share few postsynaptic partners or that the relative number of synapses onto common postsynaptic partners are different.

Hierarchical clustering of cosine similarity scores confirmed that FeCO axons of the same subtype provide similar synaptic output to the same postsynaptic partners (**Figure 2I**). FeCO axons tuned to different tibia positions (claw flexion vs. claw extension axons) or movement directions (hook flexion vs. hook extension axons) demonstrate very low (almost zero) cosine similarity scores, indicating that their postsynaptic connectivity is very different. Instead, hook and claw axons that share directional selectivity (claw and hook flexion or claw and hook extension axons) demonstrate some shared connectivity, as suggested by cosine similarity scores above zero. Unexpectedly, we found that hook flexion axons and club axons share some postsynaptic connectivity, as demonstrated by their relatively high cosine similarity scores and co-clustering. For example, one specific VNC interneuron received synaptic input from almost

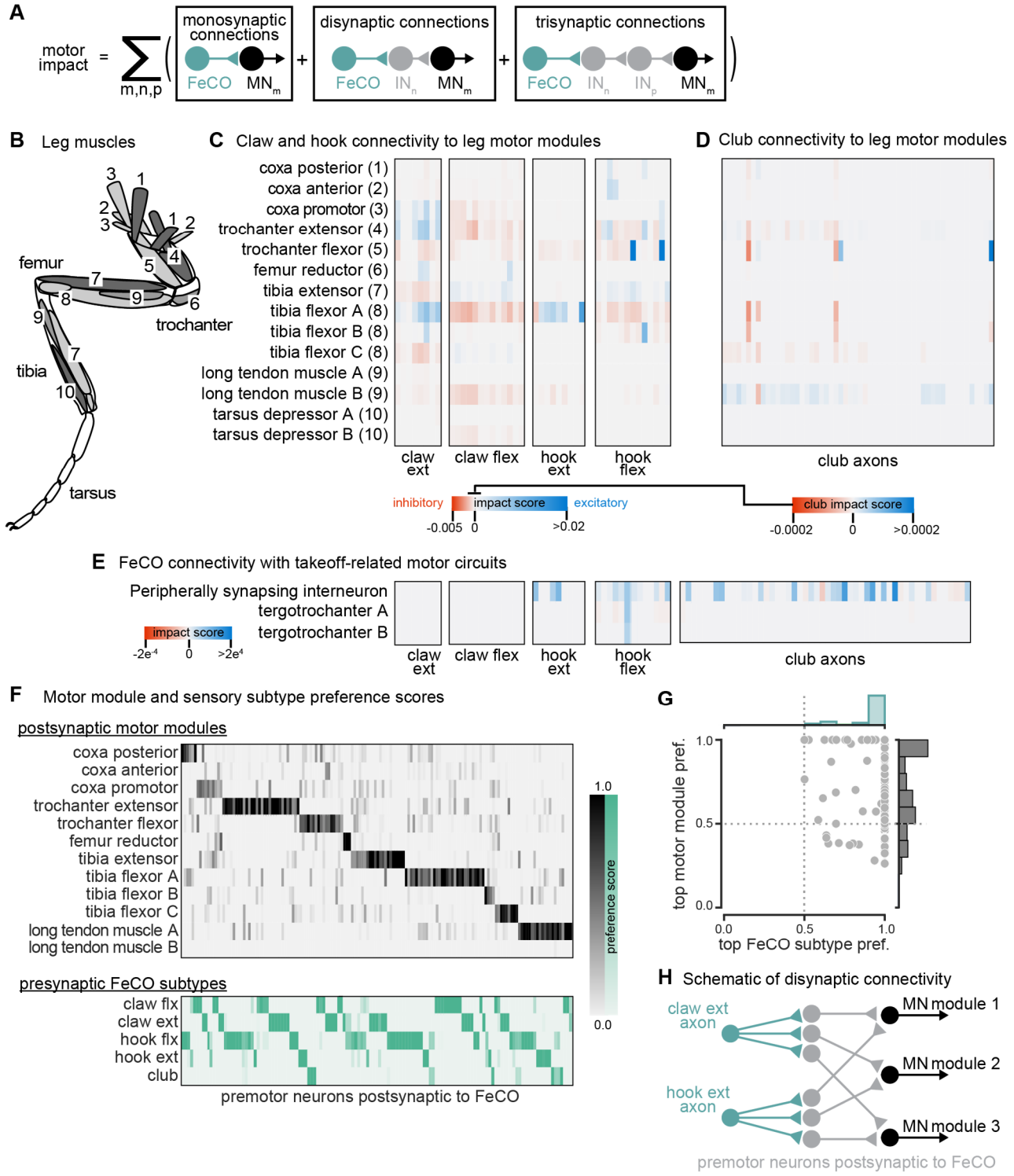

Figure 3. The connectivity of hook and claw neurons is structured to impact activity of leg motor neurons. (**A**) We developed an impact score that takes into account monosynaptic, disynaptic, and trisynaptic connections between FeCO axons and leg motor neurons (see methods). (**B**) Schematic of the 18 muscles controlling the fly's front leg. Numbers correspond to motor module labels in panel C. (**C**) Motor impact scores of claw and hook axons on leg motor modules. Motor modules are functional groupings of motor neurons that receive common synaptic input and act on the same joint[27]. The target muscles of each motor module are indicated in panel B. (**D**) Motor impact scores of club axons on leg motor modules. Note the scale bar change from panel C. (**E**) Motor impact scores of FeCO axons onto take-off related motor circuits. The peripherally synapsing interneuron is a premotor neuron involved in takeoff. The tergotrochanter is a leg muscle that is not active during walking but is instead involved in jumping and takeoff [26,43,44]. (**F**) Motor module preference scores (gray, top) and FeCO subtype preference scores (green, bottom) for each premotor VNC neuron that receives input from FeCO axons (columns). Premotor neurons are arranged according to their preferred motor module followed by their preferred FeCO subtype. (**G**) Motor module preference (y-axis) plotted against FeCO subtype preference (x-axis) for each premotor VNC neuron that receives input from FeCO axons. (**H**) Schematic representation of the predominant connectivity pattern seen between FeCO neurons and motor modules. Premotor neurons postsynaptic to the FeCO are primarily dedicated to relaying information from a particular FeCO subtype to a particular motor module.

199 all club and hook flexion axons (**Figure 2H**). We also calculated and clustered the similarity scores for
200 FeCO axons based on their synaptic inputs (**Figure S4E-F**). However, because FeCO axons have far fewer
201 (and in some cases zero) presynaptic partners (**Figure S1D,** 2.9 ± 0.3 neurons, mean ± s.e.m.), these
202 similarity scores are dominated by the shared connectivity of just a few presynaptic neurons. Claw extension
203 and claw flexion axons receive little shared synaptic input. In contrast, hook flexion and hook extension
204 axons all receive very similar synaptic input. Only a small number of club axons receive presynaptic input,
205 but those that do exhibit high similarity to one another, except for two club axons whose upstream
206 connectivity is more similar to that of hook axons.

207 In summary, FeCO axons demonstrate subtype-specific pre- and postsynaptic connectivity. FeCO
208 axons within a subtype are generally more similar in their connectivity than FeCO axons of different
209 subtypes, suggesting that information from each subtype is conveyed in parallel to different downstream
210 neurons.

211

212 **Claw and hook axons connect directly and indirectly to leg motor neurons**

213 So far, we have found that club axons synapse onto VNC neurons from different morphological
214 classes and developmental hemilineages than the claw and hook axons. This segregated connectivity
215 suggests that signals from club neurons are relayed to distinct downstream circuits with different functions
216 than claw and hook neurons. Given that club neurons are the only subtype that respond to low amplitude,
217 high frequency vibration, we hypothesized that this distinct connectivity could reflect an exteroceptive
218 function of club neurons compared to the proprioceptive function of claw and hook neurons. To explore
219 this hypothesis, we next examined how each FeCO subtype connects to leg motor circuits.

220 FeCO axons can synapse directly onto motor neurons, but they can also indirectly excite or inhibit
221 motor neurons via layers of intervening interneurons. The complexity of these feedback networks makes it
222 challenging to infer how activity of FeCO neurons could impact leg motor neurons. To understand the
223 general structure of these feedback networks, we first grouped leg motor neurons into motor modules[27]
224 (**Figure 3B**). Motor modules contain varying numbers of motor neurons that, based on their anatomy and
225 presynaptic connectivity patterns, comprise a functional motor pool that drive a similar movement (e.g.,
226 tibia extension). We next examined the connectivity between FeCO neurons and motor modules in one of
227 two ways. First, we plotted the overall number of synapses made between FeCO neurons, premotor
228 interneurons, and motor neurons, inferring the interneurons' putative neurotransmitter according to their
229 hemilineage assignment (**Figure S5**). Second, we developed an impact score metric that summarizes this
230 connectivity data in a single value by weighting direct and indirect connections between FeCO axons and
231 motor modules, as well as the putative neurotransmitters of any intervening interneurons (**Figure 3A, C-**

232 **E**). This impact score is useful to understand trends or differences in motor connectivity among different
233 subsets of FeCO neurons across multiple layers, but limited in its utility to predict neuronal activity as it
234 does not include important factors such as circuit dynamics or intrinsic neural properties.

235 Both analyses revealed that claw and hook neurons make excitatory and inhibitory connections with
236 many leg motor neurons. The pattern of their connectivity is consistent with previous recordings of motor
237 neuron activity and optogenetic manipulations in *Drosophila*[25,28]. Claw and hook flexion axons provide
238 excitatory feedback to motor neurons that extend the tibia and inhibitory feedback to motor neurons that
239 flex the tibia. Claw and hook extension axons provide excitatory feedback to motor neurons that flex the
240 tibia and strong inhibitory feedback to motor neurons that extend the tibia. Claw extension axons also
241 provide excitatory feedback to other motor modules, such as the motor neurons that move the coxa forward
242 (coxa promotor) and extend the trochanter. This connectivity suggests that FeCO feedback supports leg
243 motor synergies that span multiple leg joints.

244 Consistent with our hypothesis that club neurons do not support local leg motor control, club axon
245 connectivity with leg motor neurons is weak, demonstrated by a low impact score (**Figure 3D**, note different
246 scale bar). Club axons form no direct synapses onto leg motor neurons (**Figure S5E**). However, they do
247 indirectly and weakly connect to leg motor neurons innervating the long tendon muscle (LTM), which
248 controls substrate grip[42] (**Figure S5E, Figure 3D**). Club axons also indirectly connect to the premotor
249 peripherally synapsing interneuron (PSI) (**Figure 3E),** which excite wing power muscles during
250 takeoff[14,43,44]. This connectivity suggests a pathway by which activation of club neurons could lead to startle
251 or escape behaviors, such as freezing and take-off.

252 Finally, we analyzed the overall structure of the connectivity of FeCO axons with premotor
253 interneurons that synapse on leg MNs. We found that post-FeCO premotor interneurons primarily synapse
254 onto a single motor module (**Figure 3F-G**). This finding is consistent with previous work showing that
255 most premotor neurons preferentially connect to specific motor modules[27]. We also found that all post-
256 FeCO premotor neurons receive the majority of their synaptic input from only a single FeCO sensory
257 subtype (**Figure 3F-G**). This pattern of connectivity suggests that fly leg motor circuits have a modular
258 organization, with dedicated interneurons connecting a single FeCO subtype with a single motor module
259 (**Figure 3H**).

260

261 **Club connectivity is consistent with a putative tonotopic map of tibia vibration frequency**

262 Among the five FeCO subtypes, club axons stood out as separating into subclusters that had more
263 shared connectivity with one another than other club axons (**Figure 2I**). Past recordings of calcium activity
264 from FeCO neurons in response to tibia vibration revealed that club axons are organized tonotopically[18,19].

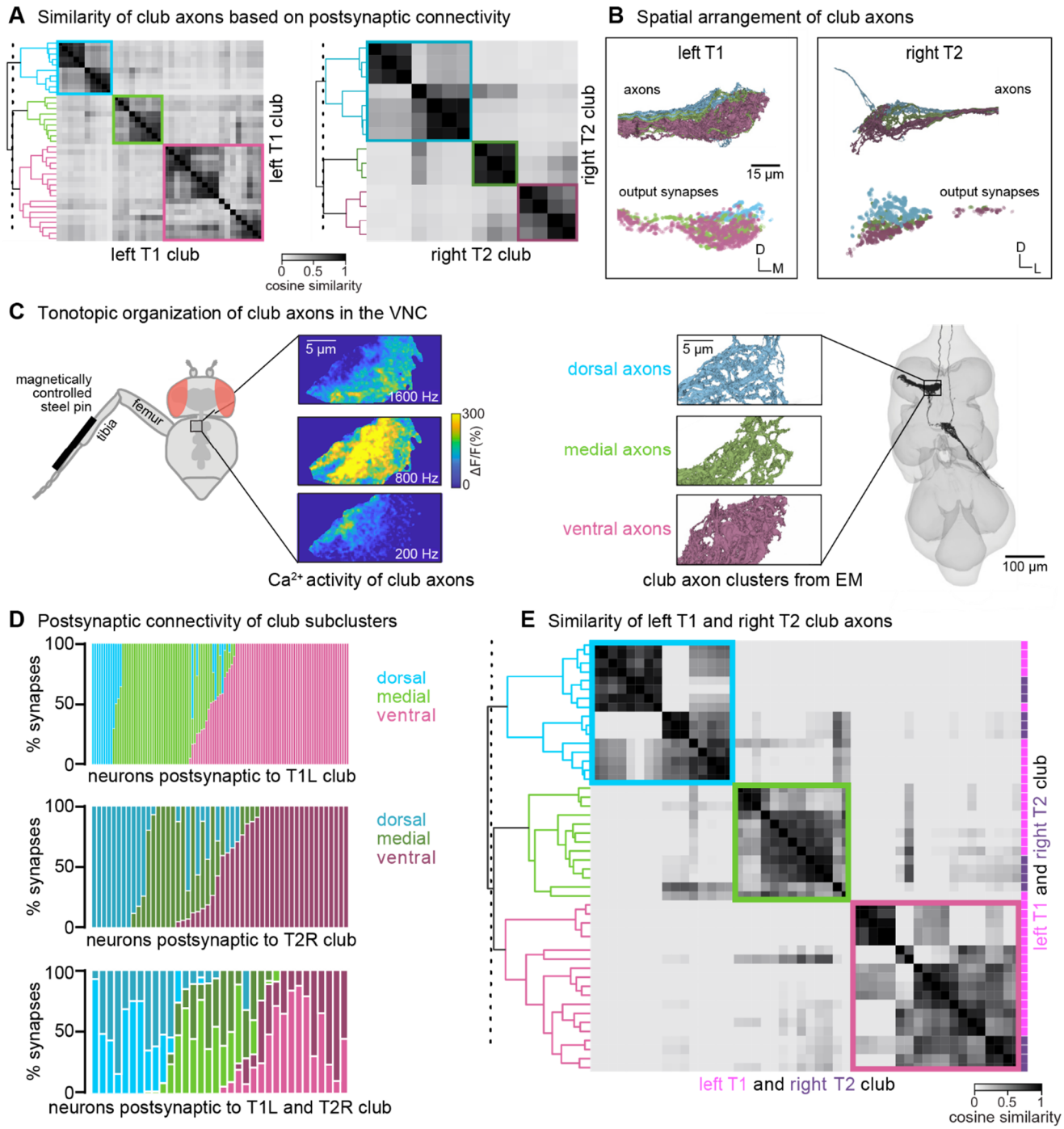

Figure 4. Club neurons cluster into spatial groups that reflect the putative tonotopic map of tibia vibration frequency. (**A**) Clustered pairwise cosine similarity matrices of the club axons based on postsynaptic connectivity. Sensory neurons with similar postsynaptic connectivity patterns cluster together, forming connectivity clusters. Left: Matrices for club axons in front left leg with connectivity clusters highlighted in blue (n = 10), green (n = 9), pink (n = 18). Right: Matrices for club axons in the middle right leg (T2R) with connectivity clusters highlighted in blue (n = 7), green (n = 3), pink (n = 4). (**B**) Top, Club axons within each connectivity cluster form 3 groups that span the dorsal-ventral axis: dorsal (blue), medial (green), and ventral (pink). Bottom, the spatial location of the output synapses for each of the club neurons color-coded by the corresponding connectivity cluster. (**C**) The dorsal-ventral organization of connectivity clusters is consistent with tonotopic mapping of tibia vibration frequency recorded from club axons with calcium imaging[15]. Left, Schematic of the experimental set-up. Calcium data from Mamiya et al., (2018) depicting calcium responses from club axons to vibration frequencies (200 Hz, 800 Hz, 1600 Hz) applied to the tibia. In this experimental setup, the club axons are imaged from a single plane with the ventral side facing the objective. Right, reconstructed club axons in the FANC dataset separated by connectivity clusters, viewed from a similar plane as the calcium data. (**D**) Fraction of input synapses from club neurons onto downstream partners. Club neurons are grouped based on connectivity cluster (dorsal: blue, medial: green, ventral: pink). (**E**) Clustered pairwise similarity matrices of the T1L (pink) and T2R (gray) club axons based on shared postsynaptic connectivity. Sensory neurons with similar postsynaptic connectivity patterns cluster together regardless of their leg of origin.

266 We therefore wondered whether the connectivity subclusters we found in the VNC connectome could
267 represent functional groupings of club axons tuned to similar vibration frequencies.

268 In support of this hypothesis, we found that the spatial organization of the connectivity subclusters
269 of club axons reflects the tonotopy observed in prior experimental recordings. We discretized the
270 connectivity subclusters into three groups (**Figure 4B**) and found that they spatially tile the dorsal-ventral
271 axis (**Figure 4B**). Previous measurements of club axon activity in response to tibia vibration revealed a
272 tonotopic map of frequency sensitivity along the anterolateral to posteromedial axis of the VNC, such that
273 the most anterolateral axons respond most strongly to low frequency vibrations and the most posteromedial
274 axons respond most strongly to high frequency vibrations[18]. Unfortunately, due to limitations in the
275 orientation of the optical path, this previous data did not measure frequency-tuning along the dorsal-ventral
276 axis. However, comparing the anatomy of the axon subclusters we reconstructed in FANC to the images of
277 calcium activity of club axons from Mamiya et al., (2018) (**Figure 4C**) suggests that the connectivity
278 subclusters represent club axons with similar frequency tuning that also synapse onto common postsynaptic
279 partners. By reconstructing an additional 14 club axons from the middle right leg (T2R), we found that this
280 spatial organization is replicated in other leg neuromeres. Club axons from this leg also separate into
281 subclusters that span the dorsal-ventral axis (**Figure 4A-B**). Finally, we found that VNC neurons
282 postsynaptic to club axons receive most of their input from club axons from the same connectivity
283 subcluster across multiple legs (**Figure 4D-E**). For example, club axons in the most dorsal subclusters of
284 the T1L and T2R legs connect to overlapping downstream partners regardless of their leg of origin.

285 In summary, we found that club axons tile the dorsal-ventral axis and demonstrate overlapping
286 postsynaptic connectivity with their immediate neighbors. We propose that individual club neurons in
287 similar locations along the dorsal-ventral axis of each leg neuromere have similar vibration frequency
288 tuning. If true, then our connectivity analyses also suggest that postsynaptic neurons integrate information
289 from club neurons with similar vibration tuning but from different legs. Thus, the putative tonotopic
290 structure observed in club axons would be preserved in postsynaptic neurons.

291

292 **Interneurons postsynaptic to club axons integrate information across legs**

293 The major downstream partners of club neurons are interneurons from the 0A/0B, 8B, 9A, and 10B
294 hemilineages (**Figure 5A**). These interneurons express different primary neurotransmitters – 8B and 10B
295 are cholinergic, whereas 0A/0B and 9A are GABAergic. They also possess distinct morphologies that imply

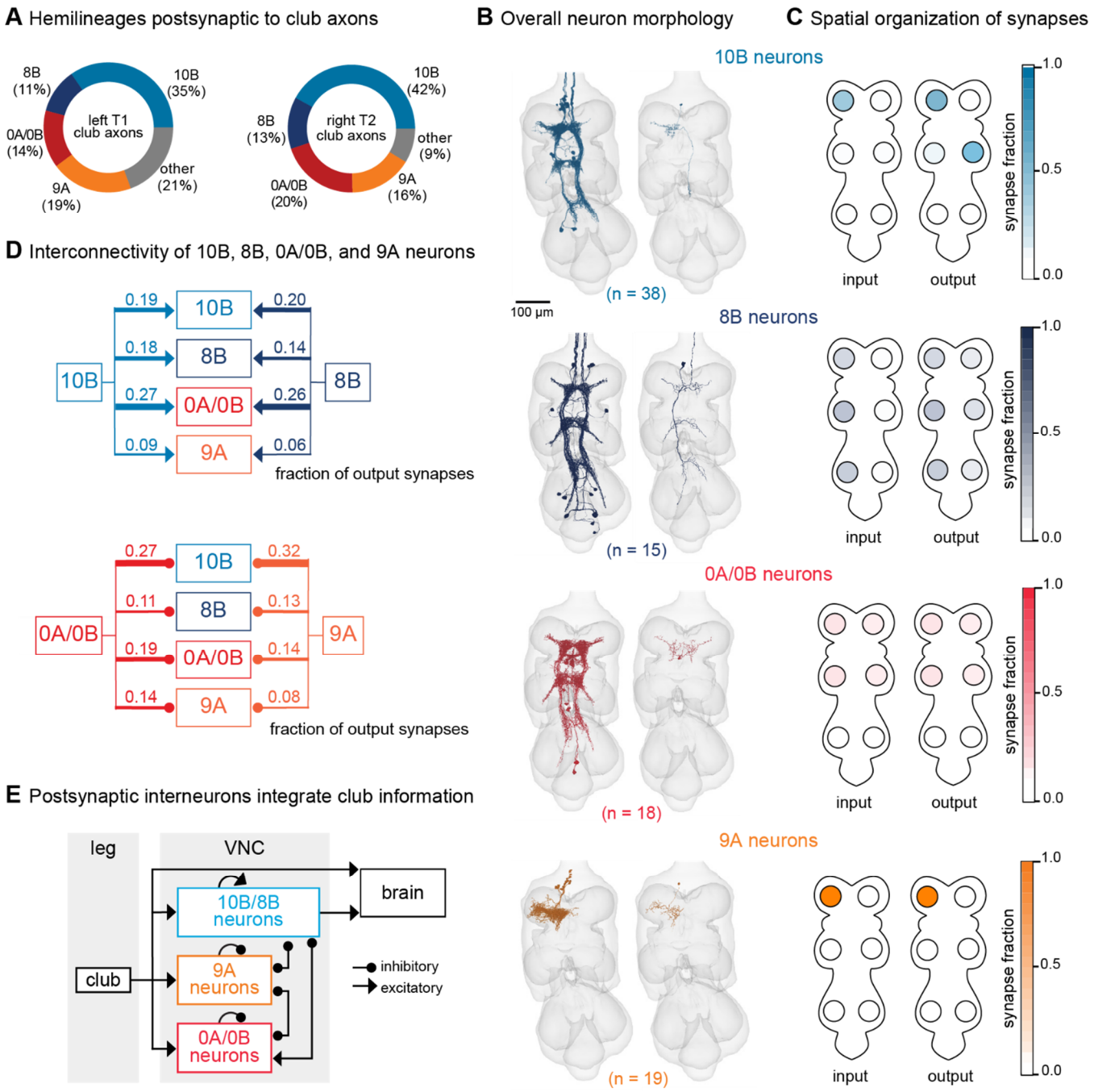

Figure 5. VNC neurons integrate vibration signals from club neurons across multiple legs. (**A**) Fraction of total output synapses from club neurons onto downstream interneurons separated by hemilineage class. 10B (light blue, n = 38), 8B (dark blue, n = 15), 0A/0B (red, n = 18). 9A (orange, n = 19) (**B**) Reconstructed interneurons downstream of left T1 club neurons from the FANC dataset. Left image shows all reconstructed neurons from each hemilineage that are downstream of T1L club neurons. Right image shows a single example neuron from that hemilineage. (**C**) Heatmap depicting the spatial locations of input (left) and output (right) synapses for 10B, 8B, 0A/0B, and 9A interneurons that are downstream of T1L club neurons. (**D**) Circuit diagram depicting recurrent connections between 10B, 8B, 0A/0B, and 9A interneurons. Each line indicates an excitatory or inhibitory connection and is labeled with the fraction of total output synapses each interneuron class makes with another interneuron class. (**E**) Schematic of the multi-layered connectivity downstream of club axons.

297 specialized roles in transforming club signals (**Figure 5B-C**). Individual 10B interneurons primarily receive
298 input from one leg and project to the contralateral and adjacent legs, whereas 8B interneurons arborize
299 broadly and have mixed input and output synapses in all six neuromeres. 0A/0B interneurons project
300 bilaterally and have pre- and post-synaptic sites on both the right and left side of each VNC segment. 9A
301 interneurons are the most localized, with their input and output synapses contained within a single
302 neuromere. The diversity of these interneuron morphologies and connectivity suggests that club information
303 is broadly relayed throughout the CNS through parallel pathways that integrate club information locally
304 within a leg and globally across multiple legs. Integration of club signals within a leg could be important
305 for amplification, while integration across legs could be important for spatial localization of vibration
306 signals. Lateral and disinhibitory circuits may sculpt vibration information, for example via normalization
307 or gain control across the population.

308 We reconstructed all 0A/0B, 8B, 9A, and 10B interneurons that receive 4 or more synapses from
309 the reconstructed T1L or T2R club neurons described above. Roughly half of the synaptic inputs onto 10B,
310 8B, 0A/0B, and 9A interneurons come directly from T1L/T2R club neurons or indirectly through their
311 downstream (second-order or third-order) partners (**Figure S6**). A much smaller fraction of inputs come
312 from other leg or wing sensory neurons or other interneurons. The remaining synaptic inputs come from
313 neurons that have not yet been proofread. Since our proofreading efforts were focused on club neurons from
314 only the T1L and T2R legs, we predict that a significant proportion of the missing input comes from club
315 neurons from other legs and their postsynaptic partners.

316 Finally, 10B, 8B, 0A/0B, and 9A interneurons downstream of club neurons exhibit high levels of
317 recurrent connectivity among interneurons from different hemilineages and different legs (**Figure 5D**).
318 Thus, the circuitry downstream of club axons is recurrent and multi-layered (**Figure 5E**). We speculate that
319 this highly interconnected circuit architecture is structured to support the capacity to localize substrate
320 vibrations in the external environment.

321

322 **Leg vibration information integrates with auditory and mechanosensory circuits in the brain**

323 Vibration signals from club neurons are relayed to the brain by ascending club axons and ascending
324 8B and 10B interneurons (**Figure 6A**). Since the FeCO has been implicated in sensing substrate vibrations
325 for courtship and escape[23,24], we hypothesized that leg vibration information carried by ascending
326 projections is integrated in the brain with sensory information from the antennae. The fly antenna also
327 contains a chordotonal organ, known as the Johnston's Organ, which detects antennal displacements and
328 local air vibrations[45–47]. To this end, we next identified where these ascending neurons project to in the
329 brain and analyzed their downstream connectivity.

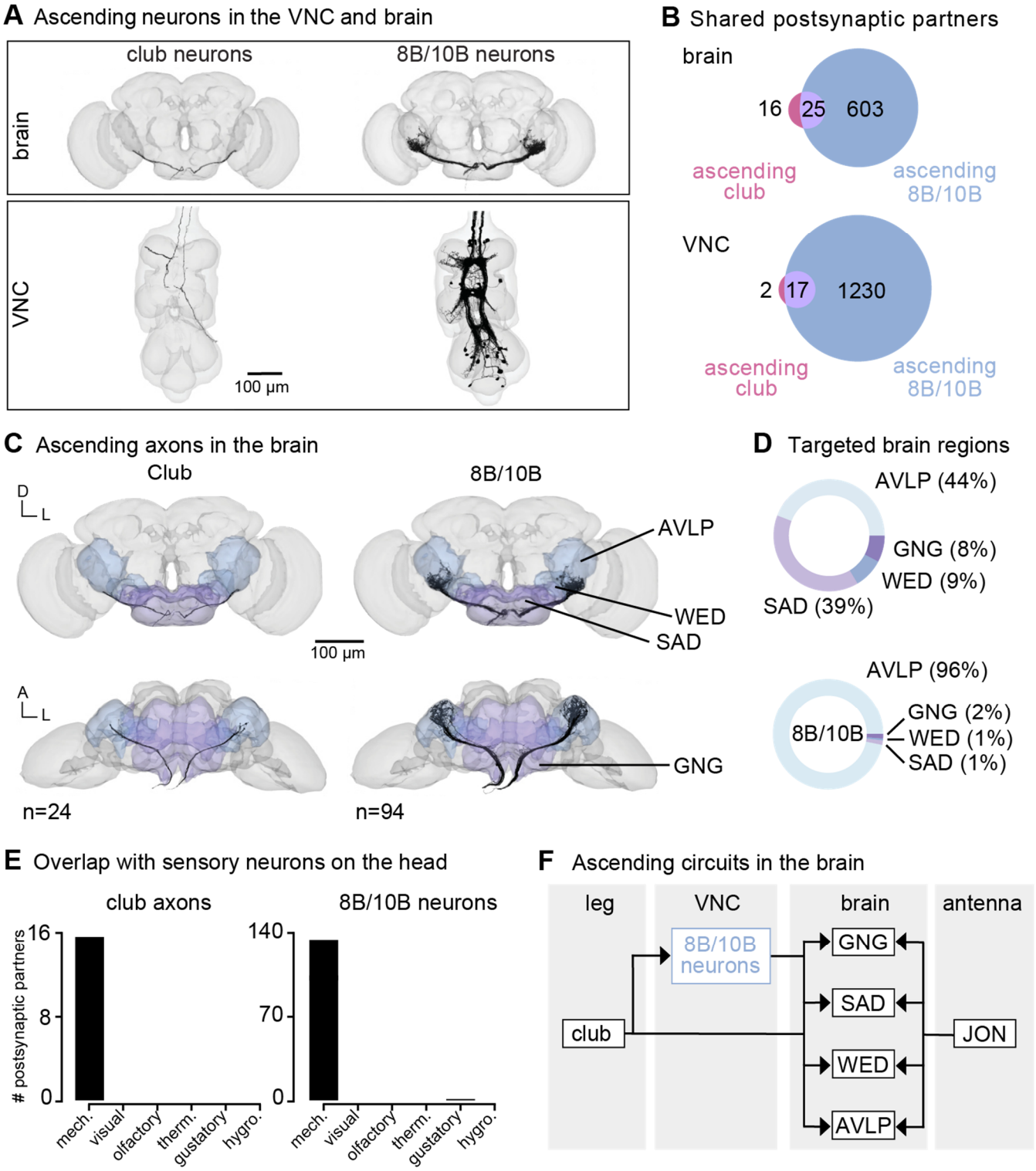

Figure 6. Vibration signals from club neurons are transmitted directly and indirectly to the brain and integrated with mechanosensory signals from the antenna. (**A**) Ascending club axons and ascending 8B and 10B interneurons that are reconstructed in the FANC (bottom, 8 club axons and 52 interneurons) and Flywire (top, 24 sensory axons and 94 interneuron axons) datasets. (**B**) Venn diagrams of shared postsynaptic partners between ascending club neurons and ascending 8B/10B neurons in the VNC (top) and brain (bottom). (**C**) Images of the ascending club axons (n = 24) and ascending 8B and 10B interneurons (n = 94) in the brain dataset with targeted brain regions highlighted (Flywire). Axons project to the anterior ventrolateral protocerebrum (AVLP), wedge (WED), saddle (SAD), and gnathal ganglion (GNG). (**D**) Percentage of synaptic outputs from ascending club axons (top) and ascending 8B/10Bs interneurons (bottom) in each brain region. The ascending club axons and ascending interneurons differ with respect to distribution of output synapse location. (**E**) Number of postsynaptic partners of ascending club axons (left) and ascending 8Bs/10Bs (right) that are shared with other sensory neurons in the brain. (**F**) Circuit diagram depicting the projection patterns of ascending club and ascending 8B/10B interneurons in the brain, which integrate with antennal mechanosensory circuits.

Within the FANC dataset, we proofread 8 ascending club axons from the T1L and T2R legs, 58 ascending 10B interneurons, and 52 ascending 8B interneurons (**Figure 6A**, bottom). We then used the FlyWire brain connectome dataset[7,15] to identify ascending projections that matched light-level morphology of ascending projections from club axons, 8B interneurons, and 10B interneurons (**Figure 6A**, top, and **Supplemental Table 3** for links to view these neurons in Neuroglancer). Within the brain connectome, we found 24 axons that matched the projections of ascending club axons and 94 axons that matched the ascending projections of 8B and 10B interneurons. Due to the similarity of their ascending projections, we could not resolve which interneuron axons belong to which hemilineage (8B or 10B) in the brain connectome. However, 8B/10B interneuron branching patterns in the brain are notably different from those of ascending club neurons. Club axons are smooth with few branches, while 8B/10B axons branch extensively.

To understand the differences between these two ascending pathways, we compared their connectivity in the VNC and the brain (**Figure 6B**). Ascending club axons and 8B/10B interneurons are interconnected and share several downstream partners in the VNC. For example, the majority of postsynaptic partners of ascending club axons in the VNC (17/19) and the brain (25/41) also receive input from ascending 8B/10B interneurons (**Figure 6B**). However, 8B/10B interneurons have many more postsynaptic partners than club neurons, thus targeting many of the same postsynaptic partners as ascending club neurons, but also several non-overlapping downstream partners.

Consistent with our hypothesis that club neurons are exteroceptive, we found that ascending club and 8B/10B neurons target brain regions that broadly integrate external sensory information: the anterior ventrolateral protocerebrum (AVLP), wedge (WED), saddle (SAD), and gnathal ganglion (GNG) (**Figure 6C-D**). The AVLP, WED, SAD, and GNG encode mechanosensory information from the antennae, including signals related to wind and courtship song[45,48–50]. Neurons in the WED encode antennal vibration, are tonotopically organized, and some even respond to high frequency antennal vibrations (>600 Hz)[45]. Ascending club neurons and 8B/10B interneurons primarily converge onto downstream partners that also receive input from other head mechanosensory neurons (**Figure 6E**), including auditory and mechanosensory Johnston's Organ neuron (JON) subtypes, mechanosensory bristles, and antennal campaniform sensilla (**Figure S7**). This shared connectivity suggests that, in the brain, neurons integrate mechanosensory information from across the body, including the legs, wings, neck, head, and antennae. We speculate that this comparison could contribute to the detection and localization of mechanical vibrations in the external environment (**Figure 6F**).

364 **Discussion**

365 Here, we used connectomic reconstruction of neural circuits to infer the function of limb
366 somatosensory neurons from patterns of synaptic connectivity. Prior experiments in *Drosophila* and other
367 insects had suggested that the femoral chordotonal organ (FeCO), serves a dual proprioceptive and
368 exteroceptive function[18–24]. Our analyses support this conclusion and suggest that each function is supported
369 by distinct FeCO sensory subtypes connected to distinct downstream circuits. Based on their connectivity,
370 position and movement-sensing claw and hook neurons are primarily proprioceptive and provide feedback
371 to local leg motor circuits. In contrast, vibration-sensing club neurons are primarily exteroceptive. Club
372 axons provide feedback to intersegmental circuits that integrate somatosensory information across multiple
373 limbs and then convey that information to the brain. These analyses demonstrate the power of connectomic
374 mapping and analysis to identify putative functions of somatosensory neurons. They also motivate future
375 work to test the function of circuits for limb proprioception and exteroception in behaving flies.

376

377 **Role of the FeCO in local leg motor control**

378 We found that movement- and position-sensing hook and claw axons synapse directly and indirectly
379 onto leg motor neurons (**Figure 3**). This connectivity is consistent with prior evidence that the FeCO
380 contributes to stabilization of leg posture[20,25,28]. We also find that claw and hook axons provide feedback to
381 motor neurons controlling movement about multiple joints, consistent with work in locusts[51] and wētās[52].

382 Proprioceptive feedback needs to be flexibly tuned to reflect behavioral demands[53]. For example,
383 during voluntary movement, proprioceptive pathways promoting stabilizing reflexes may be attenuated to
384 avoid opposing the intended movement. One possible mechanism underlying this context-dependent tuning
385 is presynaptic inhibition of sensory axons[54,55]. In support of this mechanism, we found several inhibitory
386 upstream partners of claw and hook axons (**Figure S3**). We also showed in a recent study that hook (but
387 not claw) axons are presynaptically inhibited during voluntary leg movement[29]. In addition to direct
388 feedback onto somatosensory axons, proprioceptive feedback may also be tuned via context-dependent
389 inhibition of downstream pathways.

390 Finally, we found that claw and hook axons synapse onto a small number of intersegmental and
391 ascending neurons (**Figure 2**). Intersegmental projections could relay proprioceptive information to the
392 motor circuits of other legs. However, past work suggests that feedback from the FeCO of one leg does not
393 strongly affect control of other legs – manipulating activity of FeCO neurons has little effect on inter-leg
394 coordination[56–58]. Ascending neurons that are postsynaptic to claw and hook neurons could relay leg
395 proprioceptive information to the brain to inform action selection. Calcium imaging experiments have
396 shown that many ascending neurons are active during behaviors like walking[60]. Additionally, neurons in

397 higher order visual areas and in the central complex encode walking stride, speed, and turning behavior
398 even in the absence of visual input, suggesting that they receive self-motion cues from the legs[61–63].
399
400 **Tonotopic and spatial organization of club axons**
401 Individual club neurons are tuned to specific vibration frequencies, collectively forming a tonotopic
402 map in the VNC[18]. We found that club axons are spatially organized into sub-clusters with shared
403 postsynaptic connectivity that tile the dorsal-ventral axis of the VNC (**Figure 4**). By comparing this spatial
404 organization to prior recordings of club axon activity in the VNC[18], we hypothesize that the dorsal club
405 axons respond to higher frequencies while the ventral club axons respond to lower frequencies. However,
406 actual measurements of frequency sensitivity along the dorsal-ventral axis would be necessary to confirm
407 this hypothesis. Intersegmental second-order neurons receive input from club neurons originating in
408 different legs but situated in a similar location along this dorsal-ventral axis, suggesting that this putative
409 tonotopy is conserved in downstream circuits. However, many of these second-order neurons are densely
410 interconnected. We hypothesize that this multi-layered circuit could support spatial localization of vibration
411 stimuli. Based on this hypothesis, if we were to record the activity of 10B or 8B neurons while applying
412 vibration stimuli to different locations around the fly, we would expect to find individual neurons tuned to
413 specific frequencies and spatial locations. Our reconstruction efforts here were limited to club neurons in
414 only two leg neuropils and their postsynaptic partners. However, the similarity of connectivity across the
415 T1L and T2R club circuits suggests that our findings likely hold true for the club axons from the other legs.
416
417 **Putative exteroceptive function of club neurons**
418 Our analyses support the hypothesis that club neurons primarily function as vibration-sensing
419 exteroceptors. Interestingly, the sensitivity of club neurons is similar to Pacinian corpuscle low threshold
420 mechanoreceptors (LTMRs) in mammals (40-1000 Hz). Like club neurons, Pacinian LTMRs are active
421 during a wide variety of natural behaviors, including walking and grooming, as well as during substrate
422 vibration[65]. Recent work in the mouse has found that Pacinian signals converge with auditory input from
423 the cochlea in the lateral cortex of the inferior colliculus (LCIC)[66]. LCIC neurons respond more strongly to
424 coincident vibration-auditory stimulation than to either stimulus alone. The Pacinian to LCIC circuitry in
425 the mouse resembles the club to AMMC circuitry that we describe here in the fly, suggesting that integration
426 of limb vibration and auditory signals may be a common principal of mechanosensory processing across
427 diverse animals.
428 How animals use these vibration signals in natural environments remains unclear. In *Drosophila,*
429 males produce both airborne and substrate-borne vibrations as part of courtship[67–71]. Genetic silencing of

430 FeCO neurons in female flies reduces their receptivity to male courtship song[23], suggesting that the FeCO
431 is involved in courtship. Consistent with this hypothesis, we found downstream neurons in the brain that
432 integrate vibration information from both legs and antennae (**Figure 6**). Vibration-sensitive club neurons
433 in the leg and Johnston's Organ neurons in the antennae respond to overlapping vibration frequencies[18,19,45–
434 47], but the full sensitivity range for each group has not been carefully measured. We hypothesize that the
435 integration of vibration information from the antennae and legs could inform courtship behavior by
436 providing information regarding both airborne and substrate-borne courtship communication. Importantly,
437 in this study, we reconstructed the FeCO circuits within a female VNC and brain. If club neurons support
438 detection of courtship-related signals, the circuitry downstream of the club neurons could be sexually
439 dimorphic and thus differ in male flies. Further reconstruction in the male VNC connectome (MANC)
440 would be needed to test this possibility.

441 Aside from courtship, vibration information from club neurons could also be used to detect
442 movements of predators or other threats, such as wind or rain. Consistent with this hypothesis, we found
443 that club axons are indirectly connected to escape-related neurons, including motor neurons innervating the
444 long tendon muscle (LTM) and the premotor peripherally synapsing interneuron (PSI) (**Figure 3**).
445 Activation of club neurons could promote leg freezing via activation of the LTM, or take-off via activation
446 of the PSI. Previous studies have implicated the FeCO in escape and courtship responses in multiple insect
447 species beyond *Drosophila*[21,23,24]. Crustaceans also have leg chordotonal organs that can detect external
448 substrate vibrations and which support vibration-based social communications[72–74]. Many insect species
449 also possess subgenual organs, specialized vibration sensors in the tibia, but flies lack these sensory
450 structures[64]. Thus, in *Drosophila*, club neurons are likely the primary sensors that detect substrate vibrations
451 via the legs.

452

453 **Lack of convergence across FeCO subtypes in second-order neurons**

454 We were surprised to find that the downstream connectivity of each FeCO subtype is quite distinct:
455 very few VNC neurons receive synapses from more than one FeCO subtype (**Figure 2**). Past work proposed
456 a higher degree of convergence across FeCO subtypes within second-order neurons. Using whole cell patch-
457 clamp recordings and 2-photon calcium imaging, we previously characterized multiple VNC interneuron
458 cell types that encode combinations of femur-tibia joint movement, position, and vibration, suggesting that
459 they receive input from multiple FeCO subtypes[25]. In another study, we combined optogenetic activation
460 and calcium imaging to map the functional connectivity between FeCO axons and their downstream
461 partners[26]. That study also found examples of VNC interneurons that receive inputs from more than one
462 FeCO subtype. One possible explanation for this discrepancy is that our connectome analyses

463 predominantly focused on direct connections between FeCO neurons and their synaptic partners. The
464 integration of information from multiple FeCO subtypes could be via indirect connections involving
465 multiple intervening interneurons. In addition, Agrawal et al. (2020) found evidence for mixed electrical
466 and chemical synapses that connect FeCO sensory neurons with some downstream partners. The FANC
467 EM dataset was not imaged at sufficient spatial resolution to resolve electrical synapses. Finally, we did
468 find some weak shared connectivity between FeCO cell types that share directional selectivity, such as claw
469 and hook flexion axons or claw and hook extension axons. Due to the adventitious nature of their physiology
470 experiments, Agrawal et al. (2020) and Chen et al. (2021) may have, by chance, characterized the few
471 interneurons that do indeed receive synaptic information from multiple FeCO subtypes. We did find some
472 overlap in the connectivity of hook flexion and club axons (**Figure 2**). This finding is consistent with
473 Agrawal et al. (2020), who found one cell type, 9Aa neurons, that respond to both flexion and vibration of
474 the femur-tibia joint. However, the implications of this overlap remain to be investigated. For example,
475 integrating exteroceptive and proprioceptive signals could enable the fly to determine if the source of the
476 vibration is due to movement of its leg. Alternatively, flies could concurrently sense movement and
477 vibration information from the leg to assess substrate texture.

478 In addition, we found substantial overlap in the downstream connectivity of FeCO neurons and other
479 leg proprioceptive neurons, such as campaniform sensilla (CS) and hair plates (HP) (**Figure 2E**). In fact,
480 claw and hook axons shared a larger number of downstream partners with CS or HP neurons than with other
481 FeCO subtypes. Work from stick insects and other species suggests that such multimodal input is important
482 for context-dependent control of proprioceptive reflexes[75,76]. For example, signals from load-sensing CS
483 neurons can reduce the effect of FeCO activation on leg motor neurons[75].

484

485 **Looking forward**

486 Connectome analysis is a powerful tool to generate and falsify hypotheses about circuit function.
487 Thanks to advances in serial-section electron microscopy and image segmentation, we are close to having
488 multiple connectomes of the fruit fly brain and VNC. As more neurons within these connectomes are
489 connected to specific functions, such as motor neurons that control a particular joint or sensory neurons that
490 detect specific signals, these maps become increasingly useful anatomical frameworks for generating
491 hypotheses about the neural control of behavior. Though physiological and behavioral measurements are
492 still necessary in order to determine how a circuit functions, our study illustrates how a global view of
493 synaptic connectivity can reveal organizing principles that motivate future experiments.

494

495 **Acknowledgements**

496 We thank members of the Tuthill laboratory for technical assistance and feedback on the manuscript. We
497 also thank Jasper S. Phelps, Wei-Chung Allen Lee, and the FANC community for their contributions to the
498 proofreading of the VNC connectome. We thank Leila Elabbady, Ellen Lesser, Shirin Mohammadian,
499 Gwendolyn Swannell, and Brandon Pratt for permission to use their unpublished reconstructions of sensory
500 neurons in FANC. We thank Jim Truman, David Shepherd, Haluk Lacin, and Elizabeth Marin for assistance
501 with hemilineage identification. This work was supported by a Postdoctoral Research Fellowship from the
502 Deutsche Forschungsgemeinschaft (DFG, German Research Foundation) project 432196121 to C.J.D, a
503 Searle Scholar Award, a Klingenstein-Simons Fellowship, a Pew Biomedical Scholar Award, a McKnight
504 Scholar Award, a Sloan Research Fellowship, the New York Stem Cell Foundation, and NIH grants
505 R01NS102333 and U19NS104655 to J.C.T., NIH grants K99NS117657 and R00NS117657 to S.A, and
506 NIH grant T32 NS 99578-3 to S.J.L. and J.C.T. J.C.T. is a New York Stem Cell Foundation – Robertson
507 Investigator.
508

509 **Methods**

510

511 **Key resources table**

Reagent type (species) or resource	Designation	Source or reference	Identifiers	Additional information
Deposited data	FANC connectome	Azevedo et al. (2024)	https://fanc.community	
Deposited data	FAFB/FlyWire connectome	Dorkenwald et al. (2024) Schlegel et al. (2024)	https://flywire.ai	
Software, algorithm	CAVEclient	Dorkenwald et al. (2024)	https://github.com/seunglab/CAVEclient	
Software,	neuPrint	Plaza et al.	https://neuprint.jan	

algorithm		(2022)	elia.org/	
Software, algorithm	Neuroglancer	Maitin-Shepard et al. (2021)	RRID:SCR_015631	
Software, algorithm	Python		RRID:SCR_008394	

512

513 **Reconstruction of neurons in the FANC connectome**

514 Neurons in the Female Adult Nerve Cord (FANC) electron microscopy dataset[8] were previously
515 segmented in an automated manner[14]. To manually correct the automated segmentation of our neurons of
516 interest, we used Google's collaborative Neuroglancer interface[78]. Many of the FeCO axons in T1L were
517 previously identified[8], and most of the claw and hook axons were previously partially corrected[29]. Here, we
518 identified and corrected additional claw axons as well as all club axons in T1L and T2R. Identification was
519 guided by light-level images of FeCO subtype-specific genetic driver lines[18,19]. An FeCO neuron was
520 deemed "completed" in its reconstruction if all major branches were attached as confirmed by comparison
521 to light microscopy images. All uncertain connections were double-checked by at least two experienced
522 proofreaders, and then a final check of each neuron was completed at the end to again confirm that no false
523 connections were added to a neuron and no major branches were missing.

524 To reconstruct pre- and postsynaptic partners of FeCO neurons, we identified all objects in the
525 automated segmentation that received at least 4 synapses from an FeCO neuron or made at least 3 synapses
526 onto an FeCO neuron. Synapses were detected automatically as described by Azevedo et al (2024). Past
527 work[15,30] found that applying a 3-4 synapse threshold mitigates the inclusion of false positive connections.
528 We then proofread those objects until associated with either a cell body, or an identified descending or
529 sensory process. A small number of objects were categorized as fragment segments and could not be
530 connected to a cell body or an identified descending or sensory process. We deemed a neuron as "proofread"
531 once its cell body was attached, its full backbone[79] reconstructed, and as many branches as could be
532 confidently attached. Neuron annotations were managed by CAVE, the Connectome Annotation Versioning
533 Engine[80]. We used custom Python scripts to interact with CAVE via CAVEclient[80].

534 We additionally reconstructed a subset of third-order neurons that are 2 hops away from T1L and/or
535 T2R club neurons. First, we identified all objects in the automated segmentation that receive at least 4
536 synapses from an 8B or 10B neuron that is postsynaptic to a club neuron. We chose to focus on neurons
537 postsynaptic to intersegmental 8B and 10B neurons to gain greater proofreading coverage of club circuitry
538 in other legs.

539

540 **Novel partners analysis**

541 To identify the number of new postsynaptic partners added to our dataset per each FeCO sensory neuron
542 we reconstructed, we first found all postsynaptic partners of all reconstructed T1L FeCO axons. Then, we
543 randomly sampled the FeCO neurons one at a time (without replacement) in a cumulative fashion, and
544 calculated how many novel postsynaptic partners were connected to each additional FeCO neuron. We re-
545 did this random sampling 50 times. To extrapolate the resulting curve and estimate the likely number of
546 postsynaptic partners for the entire 152 neurons in the FeCO, we used the curve_fit() function from the
547 SciPy python package to fit a logarithmic function.

548

549 **Cosine similarity scores**

550 Cosine similarity (for example, **Figure 2I**) was calculated using the cosine similarity method from the
551 scikit-learn python package. Cosine similarity scores were then hierarchically clustered using the
552 agglomerative clustering methods from the scikit-learn python package.

553

554 **Branch preference scores**

555 Using K-means, we clustered all output synapses from a given FeCO subtype based on their Euclidean
556 distance from one another. We formed 3 clusters, each of which corresponds to a major branch. We then
557 determined a branch preference score for every postsynaptic neuron by dividing the number of synapses
558 the postsynaptic neuron received from one branch by the total number of synapses it received from all
559 branches. In Figure S2A-D, we plot these preference scores on ternary plots. Each postsynaptic neuron is
560 represented by a point whose size varies according to the total number of synapses that that neuron receives
561 from that FeCO subtype. In Figure S2E, we randomly subsampled the synapses (while maintaining the
562 clusters as identified above). We then repeated the above analysis, but only plotted the strongest preference
563 scores per each postsynaptic neuron.

564

565 **Definition of cell classes**

566 Neurons pre- and postsynaptic of FeCO axons were identified as motor, sensory, ascending, descending,
567 intersegmental, or local neurons. Motor neurons have a cell body in the VNC and a process in the leg nerve.
568 These neurons were recently identified in the FANC dataset for the front left leg[14,27]. Sensory neurons have
569 a process in the leg nerve but no cell body in the VNC. Ascending neurons have a process in the neck
570 connective and a cell body in the VNC. Descending neurons have a process in the neck connective but no
571 cell body in the VNC. Intersegmental and local neurons have a cell body and all processes in the VNC. The

572 processes of intersegmental neurons spanned multiple neuromeres, whereas those of local neurons were
573 contained in a single neuromere. All pre- and postsynaptic neurons were manually checked to make sure
574 they were in the correct categories.
575
576 **Identification of hemilineages**
577 In *Drosophila*, neurons that share a developmental origin (i.e., belong to the same hemilineage) possess
578 common anatomical features[36] and release the same fast-acting neurotransmitter (e.g. GABA, glutamate, or
579 acetylcholine)[32]. We took advantage of this knowledge to identify the hemilineage of each neuron upstream
580 and downstream of FeCO axons in the FANC connectome. We first identified and grouped together local,
581 intersegmental, and ascending VNC neurons based on where their primary neurite entered into the neuropil.
582 These groups of similar primary neurites were then identified as known hemilineages using light
583 microscopy images of sparse GAL4 lines, cell body position along the dorsal-ventral axis[32,36,81,82], and
584 personal communication (James W. Truman, David Shepherd, Haluk Lacin, and Elizabeth Marin). Putative
585 neurotransmitter was then assigned by referencing Lacin et al., (2019). Not all of the clues are available for
586 all of the neurite bundles. See **Supplemental Table 2** for links to view entire populations of each
587 hemilineage in Neuroglancer, an online tool for viewing connectomics datasets[78].
588
589 **Motor impact score**
590 A presynaptic neuron's monosynaptic impact score onto a postsynaptic neuron is defined as the number of
591 synapses made by the presynaptic neuron onto the postsynaptic neuron, divided by the total number of input
592 synapses received by the postsynaptic neuron. Then, based on the presynaptic neurons' putative
593 neurotransmitter according to its hemilineage assignment, this impact score is either considered excitatory
594 (positive) or inhibitory (negative). In the fly, acetylcholine is typically excitatory, while GABA is typically
595 inhibitory[34,39,40]. Glutamate is excitatory at the fly neuromuscular junction, acting on ionotropic glutamate
596 receptors (GluRs), but is frequently inhibitory in the CNS, acting on the glutamate-gated chloride channel,
597 GluCl[41].
598 To compute the motor impact score of a given FeCO neuron onto a motor module (**Figure 3**), we
599 summed together the calculated impact scores of direct, monosynaptic connections, disynaptic connections,
600 and trisynaptic connections between the FeCO neuron and all motor neurons (MNs) within a module. The
601 impact score of monosynaptic connections between an FeCO neuron and a motor module is as described
602 above, but summed across all MNs within a module. We assume that direct FeCO input to MNs would be
603 cholinergic, and thus excitatory.

604 For the impact score of a disynaptic connection, we multiplied the monosynaptic impact score from
605 an FeCO neuron onto neurons that are postsynaptic to the FeCO and presynaptic to MNs from the specific
606 motor module (postFeCO/preMN neurons) by the impact score of those postFeCO/preMN neurons onto
607 the MNs within a module. If the postFeCO/preMN neuron was identified as cholinergic, then this disynaptic
608 impact score was considered to be excitatory/positive, and if it was identified as GABAergic or
609 glutamatergic, then it was considered to be inhibitory/negative. We then summed together all disynaptic
610 impact scores from the FeCO neuron to the MNs of a module.
611 For the impact score of a trisynaptic connection, we first found all neurons with an identified
612 hemilineage that were postsynaptic to the FeCO neuron (postFeCOs) and all neurons with an identified
613 hemilineage that were presynaptic to the MNs within the relevant module (preMNs). We then multiplied
614 the monosynaptic impact score from the FeCO neuron onto a postFeCO neuron by the impact score of the
615 postFeCO neuron onto a preMN neuron, and this was multiplied by the impact score of the preMN neuron
616 onto the MNs within a module. If both the postFeCO and preMN neurons were excitatory or both inhibitory,
617 then this trisynaptic impact score was positive. If one neuron was inhibitory and one was excitatory, then
618 this trisynaptic impact score was negative. We then summed together all trisynaptic impact scores from the
619 FeCO neuron to the MNs of a module.
620
621 **Module preference score**
622 To compute the preference score for a motor module (**Figure 3**), we summed the number of synapses onto
623 each MN within a module (as defined by Lesser et al., 2023) and divided by the total synapses onto all
624 MNs. To compute the sensory subtype preference score for a FeCO subtype (**Figure 3**), we summed the
625 number of synapses received from all FeCO neurons of a given subtype and divided by the total synapses
626 received from all FeCO neurons.
627
628 **Circuit analysis in the FAFB/FlyWire connectome**
629 To study connectivity in the brain, we used the Full Adult Fly Brain connectome (FAFB[11]) reconstructed
630 and proofread by the FlyWire community[11,15,80,83]. All data are from public release version 783.
631
632 **Identification of ascending neurons in the FAFB/FlyWire connectome**
633 First, we manually screened through the repository of Gen1 MCFO images on FlyLight[82] for candidate
634 images of VNCs that exhibit hallmark expression of the ascending club axons, ascending 8B interneurons,
635 and ascending 10B interneurons in the VNC. To identify the anatomy of the ascending projections in the
636 brain, we matched the ascending axons and interneurons in the VNC to the corresponding images in the

brain. Next, we matched the anatomy of the ascending projections in the brain based on the light-level images to the FAFB dataset using flywire.ai[83] and the Codex platform[84]. Specifically, we queried neurons classified as ascending and cholinergic[85,86], then matched candidates to the light-level images of the target neurons. See **Supplemental Table 3** for links to view the ascending neurons in Neuroglancer[78].

Software and data availability

Data presented in the paper was analyzed from the CAVE materialization v604 timestamp 1684915801.222989. Annotated connectivity matrices (**Figure 2**) will be available as Pandas data frames (https://pandas.pydata.org/) at the GitHub repository: https://github.com/sagrawal/Lee_2024. Also available at the repository are scripts to recreate the analyses and figures in the paper, as well as scripts to recreate the connectivity matrices for users authorized to interact with the CAVEclient. Links to public segmentations are available throughout the text, as well as in a document at the git-hub repository. All analysis was performed in Python 3.9 using custom code, making extensive use of CAVEclient (https://github.com/seung-lab/CAVEclient) and CloudVolume to interact with data infrastructure, and libraries Matplotlib, Numpy, Pandas, Scikit-learn, Scipy, stats-models and VTK for general computation, machine learning and data visualization. Additional code is available at https://github.com/htem/FANC_auto_recon, providing additional tutorials, code and documentation for interacting with FANC.

656 **References**

657 1. O'Connor, D. H., Krubitzer, L. & Bensmaia, S. Of mice and monkeys: Somatosensory processing in
658 two prominent animal models. *Prog. Neurobiol.* **201**, 102008 (2021).
659 2. Tuthill, J. C. & Wilson, R. I. Mechanosensation and Adaptive Motor Control in Insects. *Curr. Biol.* **26**,
660 R1022–R1038 (2016).
661 3. Turecek, J. & Ginty, D. D. Coding of self and environment by Pacinian neurons in freely moving
662 animals. *Neuron* **112**, 3267-3277.e6 (2024).
663 4. Reschechtko, S. & Pruszynski, J. A. Stretch reflexes. *Curr. Biol. CB* **30**, R1025–R1030 (2020).
664 5. Abraira, V. E. & Ginty, D. D. The Sensory Neurons of Touch. *Neuron* **79**, 618–639 (2013).
665 6. Macefield, V. G. The roles of mechanoreceptors in muscle and skin in human proprioception. *Curr.*
666 *Opin. Physiol.* **21**, 48–56 (2021).
667 7. Dorkenwald, S. *et al.* Neuronal wiring diagram of an adult brain. *Nature* **634**, 124–138 (2024).
668 8. Phelps, J. S. *et al.* Reconstruction of motor control circuits in adult *Drosophila* using automated
669 transmission electron microscopy. *Cell* **184**, 759-774.e18 (2021).
670 9. Takemura, S. *et al.* A Connectome of the Male Drosophila Ventral Nerve Cord. *eLife* **13**, (2024).
671 10. Winding, M. *et al.* The connectome of an insect brain. *Science* **379**, eadd9330 (2023).
672 11. Zheng, Z. *et al.* A Complete Electron Microscopy Volume of the Brain of Adult *Drosophila*
673 *melanogaster*. *Cell* **174**, 730-743.e22 (2018).
674 12. Hampel, S. *et al.* Distinct subpopulations of mechanosensory chordotonal organ neurons elicit
675 grooming of the fruit fly antennae. *eLife* **9**, e59976 (2020).
676 13. Kim, H. *et al.* Wiring patterns from auditory sensory neurons to the escape and song-relay pathways
677 in fruit flies. *J. Comp. Neurol.* **528**, 2068–2098 (2020).
678 14. Azevedo, A. *et al.* Connectomic reconstruction of a female *Drosophila* ventral nerve cord. *Nature*
679 **631**, 360–368 (2024).
680 15. Schlegel, P. *et al.* Whole-brain annotation and multi-connectome cell typing of *Drosophila*. *Nature*
681 **634**, 139–152 (2024).

682 16. Phillis, R., Statton, D., Caruccio, P. & Murphey, R. K. Mutations in the 8 kDa dynein light chain gene
683 disrupt sensory axon projections in the *Drosophila* imaginal CNS. *Development* **122**, 2955–2963
684 (1996).
685 17. Smith, S. A. & Shepherd, D. Central afferent projections of proprioceptive sensory neurons in
686 *Drosophila* revealed with the enhancer-trap technique. *J. Comp. Neurol.* **364**, 311–323 (1996).
687 18. Mamiya, A., Gurung, P. & Tuthill, J. C. Neural coding of leg proprioception in *Drosophila*. *Neuron*
688 **100**, 636–650 (2018).
689 19. Mamiya, A. *et al.* Biomechanical origins of proprioceptor feature selectivity and topographic maps in
690 the *Drosophila* leg. *Neuron* **111**, 3230-3243.e14 (2023).
691 20. Field, L. H. & Matheson, T. Chordotonal Organs of Insects. in *Advances in Insect Physiology* (ed.
692 Evans, P. D.) vol. 27 1–228 (Academic Press, 1998).
693 21. Eberhard, M. J. B. *et al.* Structure and sensory physiology of the leg scolopidial organs in
694 Mantophasmatodea and their role in vibrational communication. *Arthropod Struct. Dev.* **39**, 230–241
695 (2010).
696 22. Field, L. H. & Pflüger, H.-J. The femoral chordotonal organ: A bifunctional orthopteran (Locusta
697 migratoria) sense organ? *Comp. Biochem. Physiol. A Physiol.* **93**, 729–743 (1989).
698 23. McKelvey, E. G. Z. *et al. Drosophila* females receive male substrate-borne signals through specific
699 leg neurons during courtship. *Curr. Biol.* **31**, 3894-3904.e5 (2021).
700 24. Takanashi, T., Fukaya, M., Nakamuta, K., Skals, N. & Nishino, H. Substrate vibrations mediate
701 behavioral responses via femoral chordotonal organs in a cerambycid beetle. *Zool. Lett.* **2**, 18
702 (2016).
703 25. Agrawal, S. *et al.* Central processing of leg proprioception in *Drosophila*. *eLife* **9**, e60299 (2020).
704 26. Chen, C. *et al.* Functional architecture of neural circuits for leg proprioception in *Drosophila*. *Curr Biol*
705 **31**, 5163-5175.e7 (2021).
706 27. Lesser, E. *et al.* Synaptic architecture of leg and wing premotor control networks in *Drosophila*.
707 *Nature* **631**, 369–377 (2024).

708 28. Azevedo, A. W. *et al.* A size principle for recruitment of *Drosophila* leg motor neurons. *Elife* **9**,
709 e56754 (2020).
710 29. Dallmann, C. J. *et al.* Presynaptic inhibition selectively suppresses leg proprioception in behaving
711 *Drosophila*. 2023.10.20.563322 Preprint at https://doi.org/10.1101/2023.10.20.563322 (2024).
712 30. Scheffer, L. K. *et al.* A connectome and analysis of the adult *Drosophila* central brain. *eLife* **9**,
713 e57443 (2020).
714 31. Truman, J. W., Moats, W., Altman, J., Marin, E. C. & Williams, D. W. Role of Notch signaling in
715 establishing the hemilineages of secondary neurons in *Drosophila melanogaster*. *Development* **137**,
716 53–61 (2010).
717 32. Lacin, H. *et al.* Neurotransmitter identity is acquired in a lineage-restricted manner in the *Drosophila*
718 CNS. *eLife* **8**, e43701 (2019).
719 33. Eckstein, N. *et al.* Neurotransmitter classification from electron microscopy images at synaptic sites
720 in *Drosophila melanogaster*. *Cell* **187**, 2574-2594.e23 (2024).
721 34. Allen, A. M. *et al.* A single-cell transcriptomic atlas of the adult *Drosophila* ventral nerve cord. *eLife* **9**,
722 e54074 (2020).
723 35. Lacin, H. & Truman, J. W. Lineage mapping identifies molecular and architectural similarities
724 between the larval and adult *Drosophila* central nervous system. *eLife* **5**, e13399 (2016).
725 36. Harris, R. M., Pfeiffer, B. D., Rubin, G. M. & Truman, J. W. Neuron hemilineages provide the
726 functional ground plan for the *Drosophila* ventral nervous system. *eLife* **4**, e04493 (2015).
727 37. Mark, B. *et al.* A developmental framework linking neurogenesis and circuit formation in the
728 *Drosophila* CNS. *eLife* **10**, e67510 (2021).
729 38. Li, H. *et al.* Fly Cell Atlas: A single-nucleus transcriptomic atlas of the adult fruit fly. *Science* **375**,
730 eabk2432 (2022).
731 39. Gowda, S. B. M. *et al.* GABAergic inhibition of leg motoneurons is required for normal walking
732 behavior in freely moving *Drosophila*. *Proc. Natl. Acad. Sci.* **115**, E2115–E2124 (2018).

733 40. Lees, K. *et al.* Actions of agonists, fipronil and ivermectin on the predominant in vivo splice and edit
734 variant (RDLbd, I/V) of the *Drosophila* GABA receptor expressed in Xenopus laevis oocytes. *PloS*
735 *One* **9**, e97468 (2014).
736 41. Liu, W. W. & Wilson, R. I. Glutamate is an inhibitory neurotransmitter in the *Drosophila* olfactory
737 system. *Proc. Natl. Acad. Sci. U. S. A.* **110**, 10294–10299 (2013).
738 42. Zill, S. N., Chaudhry, S., Büschges, A. & Schmitz, J. Force feedback reinforces muscle synergies in
739 insect legs. *Arthropod Struct. Dev.* **44**, 541–553 (2015).
740 43. King, D. G. & Wyman, R. J. Anatomy of the giant fibre pathway in *Drosophila*. I. Three thoracic
741 components of the pathway. *J. Neurocytol.* **9**, 753–770 (1980).
742 44. Tanouye, M. A. & Wyman, R. J. Motor outputs of giant nerve fiber in *Drosophila*. *J. Neurophysiol.* **44**,
743 405–421 (1980).
744 45. Patella, P. & Wilson, R. I. Functional Maps of Mechanosensory Features in the *Drosophila* Brain.
745 *Curr. Biol. CB* **28**, 1189-1203.e5 (2018).
746 46. Ishikawa, Y., Okamoto, N., Nakamura, M., Kim, H. & Kamikouchi, A. Anatomic and Physiologic
747 Heterogeneity of Subgroup-A Auditory Sensory Neurons in Fruit Flies. *Front. Neural Circuits* **11**, 46
748 (2017).
749 47. Yorozu, S. *et al.* Distinct sensory representations of wind and near-field sound in the *Drosophila*
750 brain. *Nature* **458**, 201–205 (2009).
751 48. Matsuo, E. *et al.* Organization of projection neurons and local neurons of the primary auditory center
752 in the fruit fly *Drosophila melanogaster*. *J. Comp. Neurol.* **524**, 1099–1164 (2016).
753 49. Suver, M. P. *et al.* Encoding of Wind Direction by Central Neurons in *Drosophila*. *Neuron* **102**, 828-
754 842.e7 (2019).
755 50. Baker, C. A. *et al.* Neural network organization for courtship-song feature detection in *Drosophila*.
756 *Curr. Biol. CB* **32**, 3317-3333.e7 (2022).
757 51. Burrows, M. & Horridge, G. A. The organization of inputs to motoneurons of the locust metathoracic
758 leg. *Philos. Trans. R. Soc. Lond. B. Biol. Sci.* **269**, 49–94 (1974).

759 52. Field, L. H. & Rind, F. C. A single insect chordotonal organ mediates inter- and intra-segmental leg
760 reflexes. *Comp. Biochem. Physiol. A Physiol.* **68**, 99–102 (1981).
761 53. Azim, E. & Seki, K. Gain control in the sensorimotor system. *Curr. Opin. Physiol.* **8**, 177–187 (2019).
762 54. Koch, S. C. *et al.* RORβ Spinal Interneurons Gate Sensory Transmission during Locomotion to
763 Secure a Fluid Walking Gait. *Neuron* **96**, 1419-1431.e5 (2017).
764 55. McComas, A. J. Hypothesis: Hughlings Jackson and presynaptic inhibition: is there a big picture? *J.*
765 *Neurophysiol.* **116**, 41–50 (2016).
766 56. Chockley, A. S. *et al.* Subsets of leg proprioceptors influence leg kinematics but not interleg
767 coordination in *Drosophila melanogaster* walking. *J. Exp. Biol.* **225**, jeb244245 (2022).
768 57. Delcomyn, F. Factors Regulating Insect Walking. *Annu. Rev. Entomol.* **30**, 239–256 (1985).
769 58. Pratt, B. G., Lee, S.-Y. J., Chou, G. M. & Tuthill, J. C. Miniature linear and split-belt treadmills reveal
770 mechanisms of adaptive motor control in walking *Drosophila*. *Curr. Biol.* **34**, 4368-4381.e5 (2024).
771 59. Laurent, G. & Burrows, M. Intersegmental interneurons can control the gain of reflexes in adjacent
772 segments of the locust by their action on nonspiking local interneurons. *J. Neurosci. Off. J. Soc.*
773 *Neurosci.* **9**, 3030–3039 (1989).
774 60. Chen, C.-L. *et al.* Ascending neurons convey behavioral state to integrative sensory and action
775 selection brain regions. *Nat. Neurosci.* **26**, 682–695 (2023).
776 61. Cruz, T. L. & Chiappe, M. E. Multilevel visuomotor control of locomotion in *Drosophila*. *Curr. Opin.*
777 *Neurobiol.* **82**, 102774 (2023).
778 62. Fujiwara, T., Brotas, M. & Chiappe, M. E. Walking strides direct rapid and flexible recruitment of
779 visual circuits for course control in *Drosophila*. *Neuron* **110**, 2124-2138.e8 (2022).
780 63. Pfeiffer, K. & Homberg, U. Organization and functional roles of the central complex in the insect
781 brain. *Annu. Rev. Entomol.* **59**, 165–184 (2014).
782 64. Virant-Doberlet, M., Stritih-Peljhan, N., Žunič-Kosi, A. & Polajnar, J. Functional Diversity of
783 Vibrational Signaling Systems in Insects. *Annu. Rev. Entomol.* **68**, 191–210 (2023).
784 65. Turecek, J. & Ginty, D. D. Coding of self and environment by Pacinian neurons in freely moving
785 animals. 2023.09.11.557225 Preprint at https://doi.org/10.1101/2023.09.11.557225 (2023).

786 66. Huey, E. L. *et al.* The auditory midbrain mediates tactile vibration sensing. *bioRxiv*
787 2024.03.08.584077 (2024) doi:10.1101/2024.03.08.584077.
788 67. Ewing, A. W. & Bennet-Clark, H. C. The Courtship Songs of *Drosophila*. *Behaviour* **31**, 288–301
789 (1968).
790 68. Kamikouchi, A. *et al.* The neural basis of *Drosophila* gravity-sensing and hearing. *Nature* **458**, 165–
791 171 (2009).
792 69. Murthy, M. Unraveling the auditory system of *Drosophila*. *Curr. Opin. Neurobiol.* **20**, 281–287 (2010).
793 70. Shorey, H. H. Nature of the Sound Produced by *Drosophila melanogaster* during Courtship. *Science*
794 **137**, 677–678 (1962).
795 71. Fabre, C. C. G. *et al.* Substrate-Borne Vibratory Communication during Courtship in *Drosophila*
796 *melanogaster*. *Curr. Biol.* **22**, 2180–2185 (2012).
797 72. Burke, W. An Organ for Proprioception and Vibration Sense in *Carcinus maenas*. *J. Exp. Biol.* **31**,
798 127–138 (1954).
799 73. Cohen, M. J. The crustacean myochordotonal organ as a proprioceptive system. *Comp. Biochem.*
800 *Physiol.* **8**, 223–243 (1963).
801 74. Salmon, M., Horch, K. & Hyatt, G. Barth's myochordotonal organ as a receptor for auditory and
802 vibrational stimuli in fiddler crabs (Uca pugilator and U. minax). *Mar. Freshw. Behav. Phy* **4**, 187–194
803 (1977).
804 75. Gebehart, C., Hooper, S. L. & Büschges, A. Non-linear multimodal integration in a distributed
805 premotor network controls proprioceptive reflex gain in the insect leg. *Curr. Biol. CB* **32**, 3847-
806 3854.e3 (2022).
807 76. Gebehart, C. & Büschges, A. The processing of proprioceptive signals in distributed networks:
808 insights from insect motor control. *J. Exp. Biol.* **227**, jeb246182 (2024).
809 77. Plaza, S. M. *et al.* neuPrint: An open access tool for EM connectomics. *Front. Neuroinformatics* **16**,
810 896292 (2022).
811 78. Maitin-Shepard, J. *et al.* google/neuroglancer: Zenodo https://doi.org/10.5281/zenodo.5573294
812 (2021).

79. Schneider-Mizell, C. M. *et al.* Quantitative neuroanatomy for connectomics in *Drosophila*. *eLife* **5**, e12059 (2016).

80. Dorkenwald, S. *et al.* CAVE: Connectome Annotation Versioning Engine. *bioRxiv* 2023.07.26.550598 (2023) doi:10.1101/2023.07.26.550598.

81. Marin, E. C. *et al.* Systematic annotation of a complete adult male *Drosophila* nerve cord connectome reveals principles of functional organisation. *eLife* **13**, (2024).

82. Meissner, G. W. *et al.* A searchable image resource of *Drosophila* GAL4 driver expression patterns with single neuron resolution. *eLife* **12**, e80660 (2023).

83. Dorkenwald, S. *et al.* FlyWire: online community for whole-brain connectomics. *Nat. Methods* **19**, 119–128 (2022).

84. Matsliah, A. *et al.* Neuronal parts list and wiring diagram for a visual system. *Nature* **634**, 166–180 (2024).

85. Eckstein, N. *et al.* Neurotransmitter Classification from Electron Microscopy Images at Synaptic Sites in *Drosophila Melanogaster*. 2020.06.12.148775 Preprint at https://doi.org/10.1101/2020.06.12.148775 (2023).

86. Heinrich, L., Funke, J., Pape, C., Nunez-Iglesias, J. & Saalfeld, S. Synaptic Cleft Segmentation in Non-isotropic Volume Electron Microscopy of the Complete *Drosophila* Brain. in *Medical Image Computing and Computer Assisted Intervention – MICCAI 2018* (eds. Frangi, A. F., Schnabel, J. A., Davatzikos, C., Alberola-López, C. & Fichtinger, G.) 317–325 (Springer International Publishing, Cham, 2018). doi:10.1007/978-3-030-00934-2_36.